



Sub-wavelength and non-periodic holes array based fully lensless imager

Aviram Gur^a, Ran Aharoni^a, Zeev Zalevsky^{a,*}, Vladimir G. Kutchoukov^b, Vicente Mico^c, Javier Garcia^c, Yuval Garini^d

^a School of Engineering and Nanotechnology Institute, Bar-Ilan University, Ramat-Gan 52900, Israel

^b Department of Imaging Science and Technology, Delft University of Technology, Lorentzweg 1, 2628 CJ Delft, The Netherlands

^c Departamento de Óptica, Universitat de Valencia, C/Dr. Moliner, 50, 46100 Burjassot, Spain

^d Physics Department and Nanotechnology Institute, Bar-Ilan University, Ramat-Gan 52900, Israel

ARTICLE INFO

Article history:

Received 23 July 2010

Received in revised form 24 March 2011

Accepted 28 March 2011

Available online 11 April 2011

Keywords:

Fourier transform optics

Image processing and restoration

Nano-plasmonics

ABSTRACT

We present a novel concept for microscopic imaging. The proposed microscope-like device does not include an objective lens neither a condenser. Instead, a metallic plate of sub-wavelength hole-array with a varying pitch is used to illuminate the inspected object that is mounted very close to it. As a result, the transmitted spectrum through each hole differs from the others and therefore, each spot of the detected object is illuminated with a unique spectrum. By measuring a single spectrum that is the sum of all the spectra that are transmitted through the sample and by using spectral decomposition algorithms, the spatial transmission pattern of the object can be extracted.

© 2011 Elsevier B.V. All rights reserved.

1. Introduction

In this paper we introduce a novel technique that can be used for the construction of a microscope. The main modification is introduced by replacing the lenses of the conventional microscope with a unique nano holes array and a spectrometer. In order to understand the proposed principle of operation let us first introduce the extraordinary effect of transmission of light through sub wavelength holes array.

The phenomenon was discovered in 1998 [1] and immediately became an intensive research field [2]. In these studies, it was found that the transmission through metallic array of sub wavelength holes presents three extraordinary properties:

1. It generates non diffractive features passing through the holes having extended depth of focus i.e. smaller diffraction angular span in comparison to the angular span that a regular hole with such dimensions would have had.
2. The overall transmission of the light's energy through the holes is larger than the effective energy that falls on the holes area.
3. The transmitted diffraction pattern strongly depends on the wavelength and therefore the spectral selectivity is high.

The non-diffractive pattern most likely results from interference of the light passing through the holes and surface plasmons (SPs) that

are excited in between the holes. SP effects are also responsible for the absorption of some of the illumination light. Therefore, some of the illumination that falls on the blocked areas between the holes is not lost but rather converted and redirected into radiating beams through the holes and interfering among themselves to create a non diffractive beam (beam with extended depth of focus) [3–5].

Optical microscopy constantly improves the spatial resolution in order to gain more information on the studied objects. A large variety of methods were developed in the last decade for that purpose with an ever growing number of improvements. These allow combining high resolution measurements with the observation of multiple colors (and entities), observation of living cells and three dimensional imaging, to name a few [6]. It is used for a variety of applications in biology, chemistry, material science and engineering [7,8]. Some of the most popular techniques include confocal microscopy [9], 4pi microscopy, saturation emission depletion microscopy (STED) [10], structured illumination [11] and STORM (stochastic optical reconstruction microscopy) or PALM (photo-activated localization microscopy) [12,13]. These methods have succeeded to bypass the diffraction limit and achieve spatial resolution of sub-wavelength features down to few tens of nm [8] while some of those microscope techniques require the appropriate labeling of the specimen.

In this manuscript we aim to apply significant simplification in the structure of a microscope and its additional functionalities while preserving the required imaging capabilities. We do not intend to go to the sub wavelength regime but rather to simplify the fundamental structure of the microscope by generating imaging capabilities without the need for using objective or condenser lenses.

* Corresponding author. Tel.: +972 3 5317055; fax: +972 3 7384051.
E-mail address: zalevsz@biu.ac.il (Z. Zalevsky).

The first experimental proof of the field pattern was obtained recently [14]. There the authors have illuminated a photoresist layer through a nano holes array and developed the resist. The obtained result clearly showed that the anticipated non diffractive interference pattern can be observed.

In this paper we aim to incorporate a unique holes array with a varying pitch for realizing imaging microscopy. Since the field pattern transmitted through the holes array is obtained due to interference between hundreds of light sources, it is very selective in wavelengths and results in a well-defined transmission spectrum that depends on the hole-array material, pitch and geometry. Because of the varying pitch of the holes array, illuminating the array with white light generates spatially dispersed or spatially varying spectrum that at every point depends primarily on the local pitch. This effect encodes the spatial information of the object by different spectra. The information is then collected using a single detector and analyzed by a spectrometer to find the transmitted spectrum which is decoded to provide the spatial information of the object. It should be emphasized that the system can work with a single-point detector that measures a

single spectrum that is transmitted through the complete hole-array and through the sample.

Wavelength coding was demonstrated before for coding and decoding of spatial information [15,16] as well as for microscopy [17]. Although no objective lens was used in the microscopic configuration of Ref. [17], a high quality condenser was still required in order to generate high quality dispersion of color for the space encoding. In contrast to the work of Ref. [17], in this paper we use non periodic holes array to perform the spectral dispersion and thus the newly constructed proposed microscope does not contain an objective lens (as in Ref. [17]) neither a condenser. In addition to having a fully lensless microscope the proposed configuration has the advantage that the imaging capability is obtained at very short distance from the hole array, in contrast to the method presented in Refs. [16,17] that used a chromatic dispersion element. This feature impacts the compactness of the proposed module.

A lensless method was demonstrated before [18] using a micro-fluidic chip. By moving the object across a set of holes that are aligned along a line that has a certain angle with respect to the moving object,

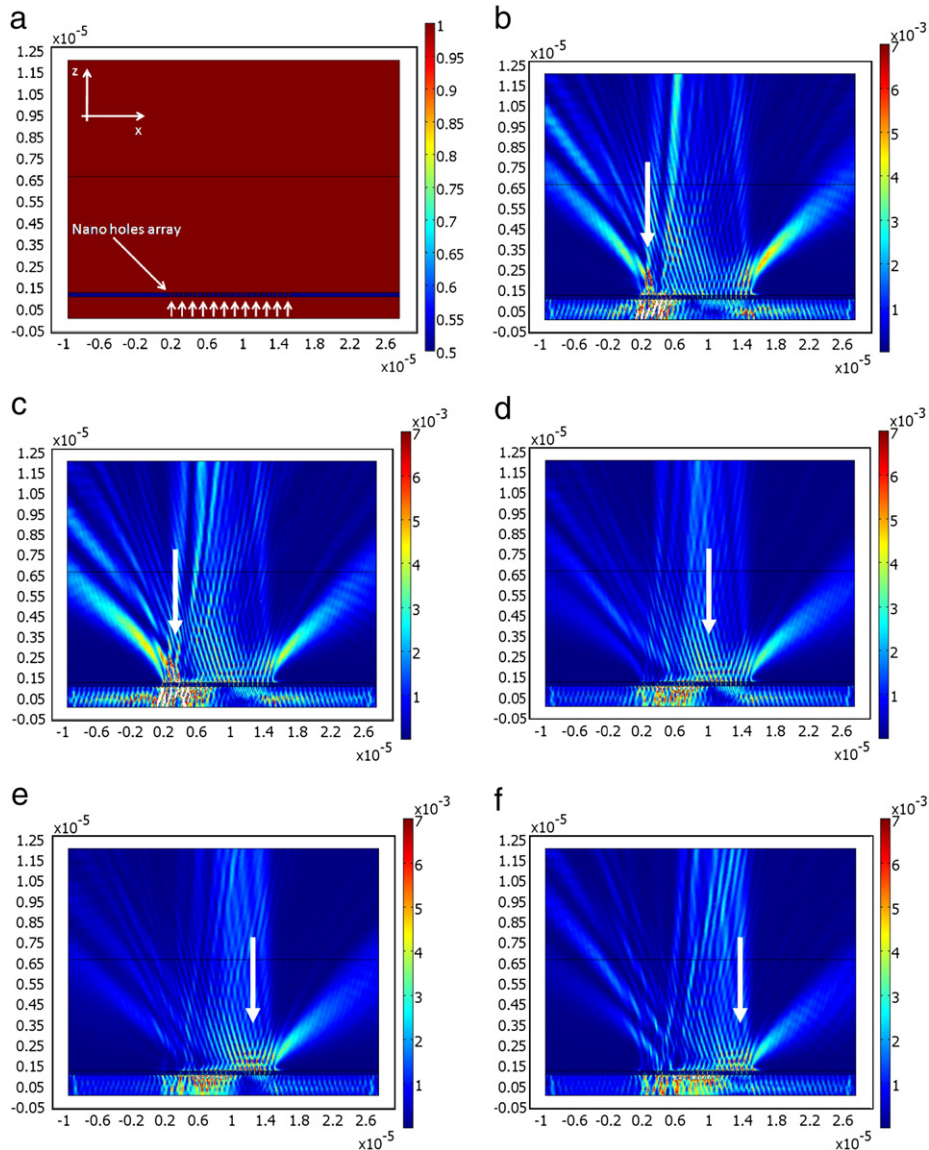


Fig. 1. Numerical simulations of non periodic and wavelength sensitive sub wavelength holes array. (a) The nano holes array where the period of the holes was monotonically varied from 500 nm on the left to 600 nm on the right in steps of 20 nm. (b–f) The field pattern when illuminating the structure with different wavelengths of b: 540, c: 550, d: 560, e: 570 and f: 580 nm. The units along all axes are in meters. The white arrows point to the hole-array region that transmits the maximal intensity.

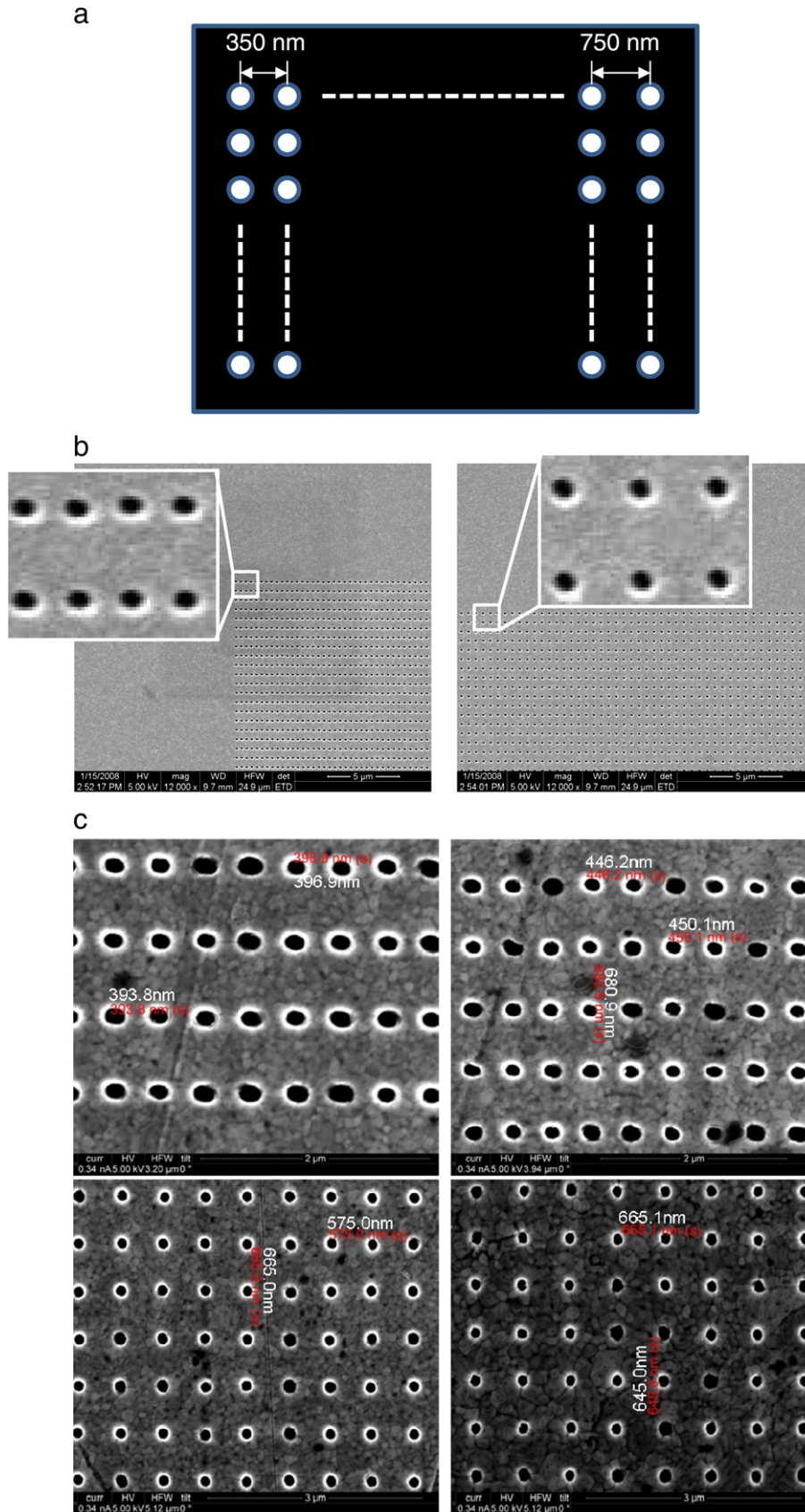


Fig. 2. (a) Schematic sketch of the holes array. (b) SEM image of the fabricated non periodic array of holes. Each hole has a diameter of 150 nm. The varying pitch is observed along the horizontal axis. It varies from 350 nm–750 nm. (c) SEM measurements performed at different locations along the array plate with measured horizontal pitch varying as 396 nm, 446 nm, 575 nm and 665 nm.

the image can be built. This method is relevant for biological samples, as scanning in a fluidic environment is crucial. Another method [19,20] demonstrates a lensless microscope while using a sample that is coupled directly to a CCD through an on-chip fiber optic faceplate and therefore reduces the spatial diffraction of the image. The microscope was demonstrated for both transmission and fluorescent samples by combining it with total internal reflection illumination setup. However, both methods still require measuring the intensity through each of the holes (or many pixels) separately, unlike the method presented here, where in principle a single-point detector is sufficient.

The holes array element can be fabricated using focused ion beam system and easily be incorporated into a mid field microscopic configuration [21].

The paper is constructed as follows: in Section 2 we describe the proposed configuration and demonstrate numerical simulations of the system. Preliminary experimental results are presented in

Section 3 while in Section 4 we describe future developments for microscopy related applications. The paper is concluded in Section 5.

2. Configuration description and numerical simulations

Due to the fact that the spectrum transmitted through the hole array with a varying pitch, we expect that the transmitted spectrum will depend on the position along the array. Thus, when illuminating a sample with white light, the element generates spatial-dependent spectra. This separation allows encoding of the spatial information of the object. The spatial information is mixed together while collected by a single pixel detector and analyzed using spectral decomposition algorithms, which decodes the spatial information from the wavelength domain back to the spatial domain. The obtained reconstruction presents a high resolution imaging configuration that does not contain an objective lens or a condenser. The main advantage of the

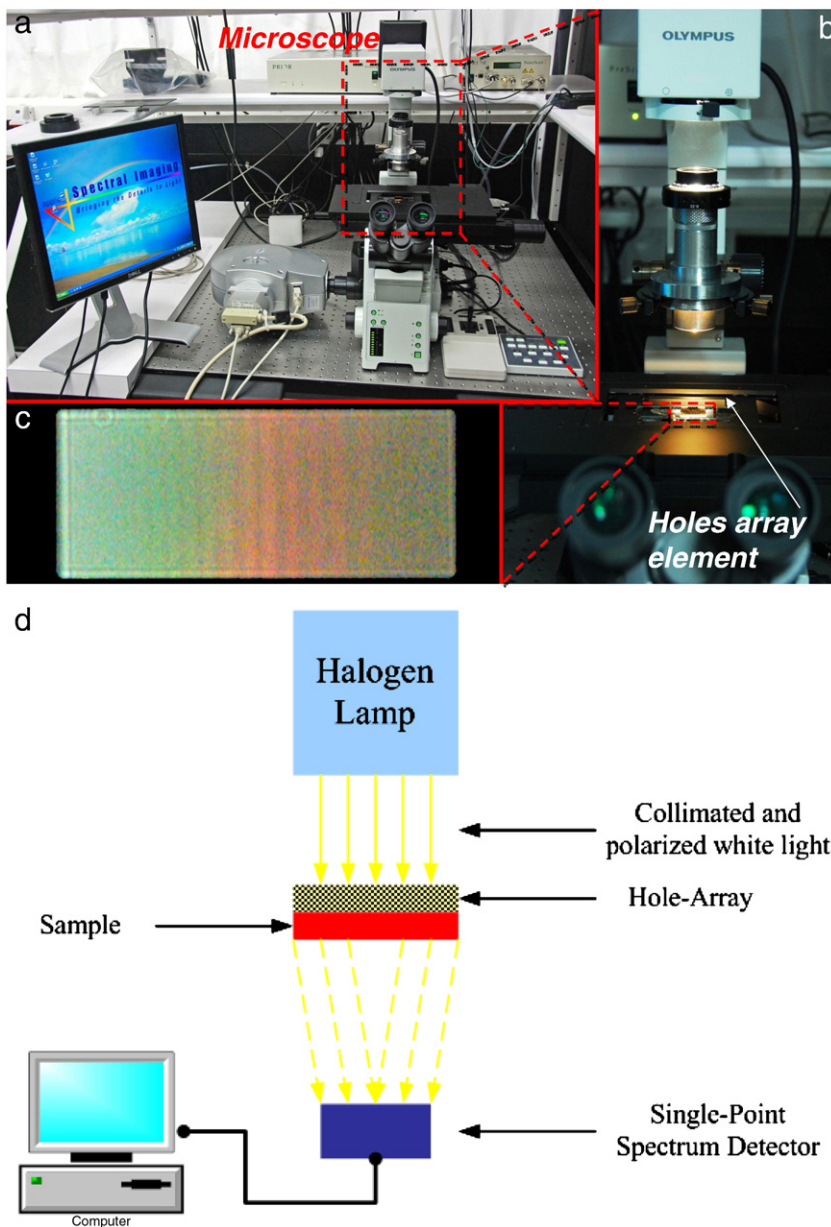


Fig. 3. Preliminary experimental demonstration. (a) Microscope station in which we positioned the fabricated non periodic holes array. (b) Collimated and polarized white light halogen lamp that is used to illuminate the fabricated element. (c) The image as observed with a microscope after illuminating the element with white halogen lamp light. (d) Schematic diagram of the optical system.

metallic holes array is its energy efficiency that allows producing high throughput even though the actual hole diameter is rather small.

Fig. 1 presents preliminary two dimensional (2D) numerical simulations demonstrating the spectral dispersing property of the proposed nano holes array. The simulation that was performed using COMSOL software solves Maxwell equations for radiation propagation using Finite Elements Method (FEM). The array is illuminated with a collimated plane wave from the bottom propagating upwards. The holes array with the varying pitch is located 1 μm above the lower edge of the figure.

All parts of Fig. 1 show the cross section in the x - z plane. Fig. 1(a) shows the nano holes array where the period of the holes was monotonically varied from 500 nm up to 600 nm in steps of 20 nm. The position of the metal plate and the direction of illumination are marked with arrows. Fig. 1(b)–(f) shows the simulation for the resulted field distribution in the x - z cross section while illuminating the nano holes array with different wavelengths varying from 540 nm (Fig. 1(b)) up to 580 nm (Fig. 1(f)) in steps of 10 nm. As one can see, the main part of the transmitted pattern (emphasized with a white arrow) is shifted from the left to the right part of the x - z plane, which demonstrates the spatial selectivity that depends mainly on the local pitch of the hole array. Note that the vertical units (z axis) in all figures are in tens of microns and thus from the results one may see that there is an axial region in which the diffracted light has extended depth of focus and within this range the spectrum is more or less uniform. Therefore, although the inspected object needs to be close to the holes array, a distance of up to few microns is sufficient, which is feasible.

3. Fabrication and preliminary experimental validation

The non periodic holes array from the numerical demonstration of Fig. 1 was fabricated using a focused ion beam (FIB) system on an area of 60 μm (vertical) by 150 μm (horizontal) with a varying pitch along the horizontal axis. The scanning electron microscope (SEM) image of the element is presented in Fig. 2. Each hole has a diameter of 150 nm and the pitch varies from 350 nm to 750 nm. The hole size does not have a significant effect on the transmitted spectrum which is determined mainly by the type of metal and the hole-spacing [21,22]. In addition, small variations from the circular shape as can be seen in Fig. 2(c) do not affect the transmitted spectrum.

The fabricated element was placed in an IX81 Olympus microscope (Fig. 3(a)) and illuminated with collimated and polarized white light from a halogen lamp (Fig. 3(b)). The spectral data was measured using the Spectracube (Applied Spectral Imaging, Migdal HaEmek, Israel) spectral imaging system that measures the transmitted spectrum at every point of the image. Although the system can work with a single-point detector that measures a single spectrum that is transmitted through the sample, for analyzing the system we used here a spectral imaging system that measures the full visible transmitted spectrum at every pixel. Fig. 3(c) shows the dispersion of colors that was measured using a CFW-1308C Scion color camera, as anticipated by the theory and by the numerical simulations previously discussed. Fig. 3(d) shows a schematic description of the system that presents the main elements of the system.

The transmission of white light through the element was measured by using the spectral imaging system. Fig. 4(a) shows a set of few measured spectra that were selected along the long axis of the element. The observed spectral shifts result from the different pitch of the hole array along the long axis of the array. Fig. 4(b) shows the peak-wavelength of each spectrum as a function of its position along the long axis of the array element. It demonstrates the concept of the holes array with the varying pitch and the ability to use it for obtaining a unique and spatial-dependent spectrum along one of the array axes.

The results shown in Fig. 4(b) can be explained by the expected transmission of light through such a metal hole-array. The transmission is allowed when the coupling of the incident light and electron

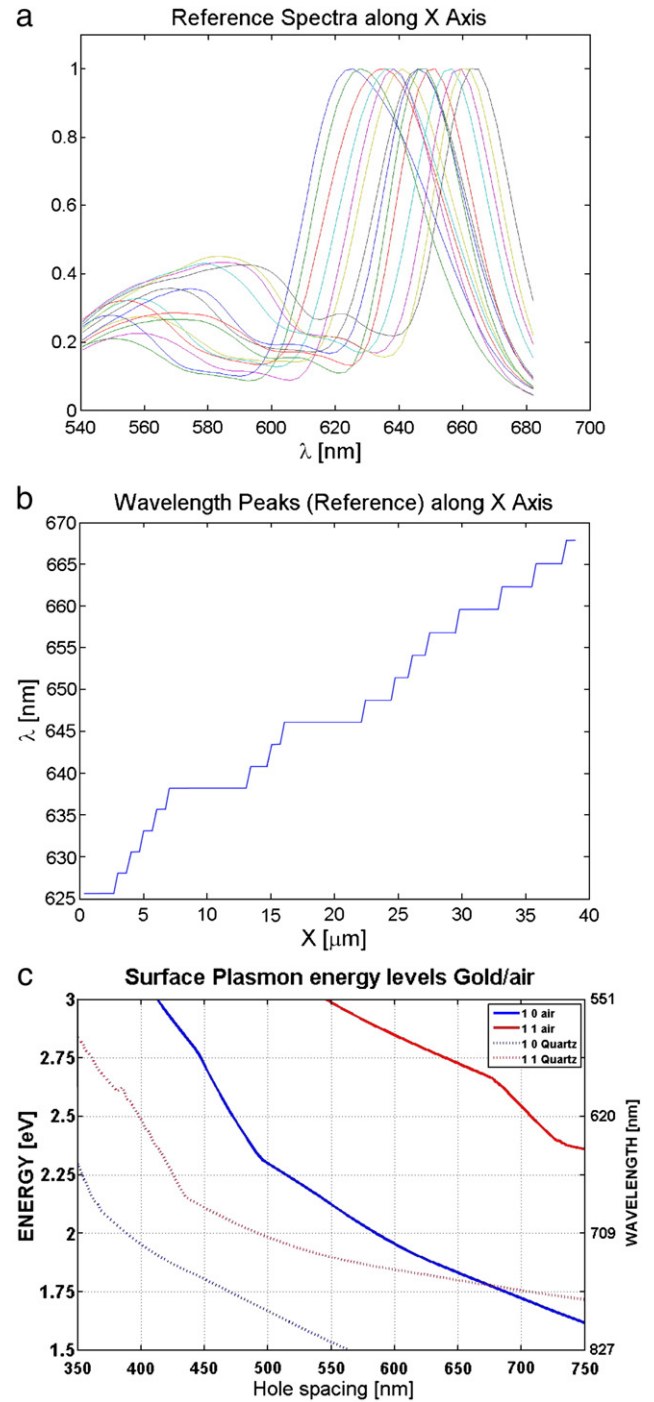


Fig. 4. Spectral transmission as measured through the holes array device. (a) An example of spectra as measured along the non periodic axis of the device. The different colors refer to different spatial positions. (b) Wavelength peaks versus spatial position along the non-periodic axis of the array. (c) Theoretical computation of the spectrum transmitted through a holes array as a function of the array pitch. The graph shows the peak transmitted energy (left axis) and wavelength (right axis) as a function of the hole-spacing. The four graphs show gold–air and gold–quartz interfaces and two different sets of quantum numbers (see text).

oscillations in the metal, or plasmons, fulfills the expected conservation of energy and momentum. The conservation of momentum requires that

$$\vec{k}_{sp} = \vec{k} + i\vec{C}_x + j\vec{C}_y \quad (1)$$

where \vec{k}_{sp} is the wave vector of the surface plasmon, \vec{k} is the component of the incident wave vector that is parallel to the hole-

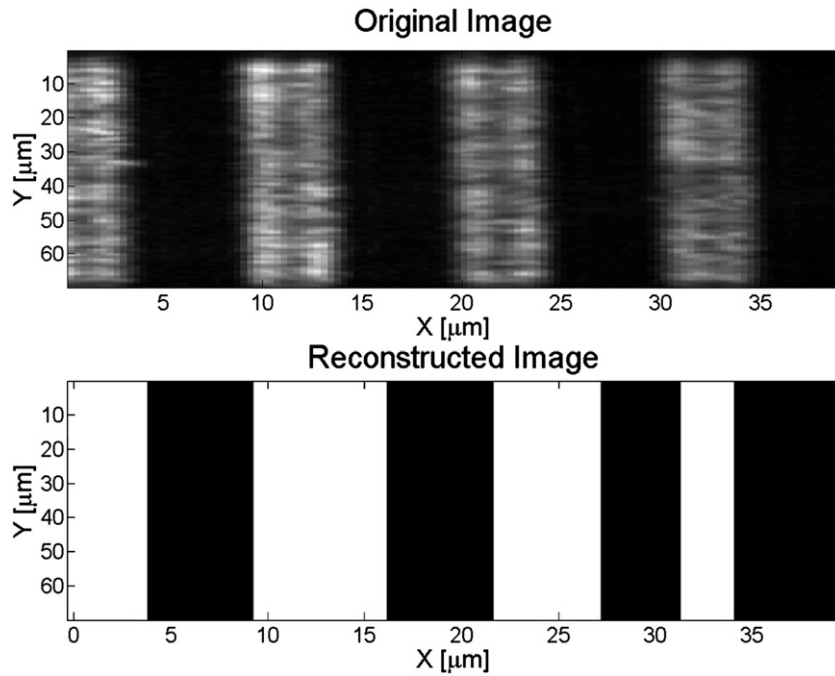


Fig. 5. Experimental results including mapping of grating of 100 lp/mm. The top is the original object captured using regular microscope having objective and condenser lenses. The bottom is the obtained reconstruction using the proposed lensless microscopic system.

array plane, \vec{G}_x and \vec{G}_y are the wave vectors of the holes array, $\vec{G}_x = 2\pi/a_0$, $\vec{G}_y = 2\pi/b_0$, where a_0 and b_0 are the array constants (pitch) along x and y and i, j are integer quantum numbers [22]. The surface plasmon wave vector is assumed to be that of a uniform metal surface that is not affected by the holes [23]:

$$k_{sp} = \frac{\omega}{c} \sqrt{\frac{\epsilon_1 \cdot \epsilon_2}{\epsilon_1 + \epsilon_2}} \quad (2)$$

where ω is the wave frequency, c the speed of light and ϵ_1 and ϵ_2 are the dielectric constants of the interface material and metal in correspondence. Substituting the plasmon wave vector from Eq. (2) in Eq. (1) and assuming that the illumination light is perpendicular to the holes array surface finally gives:

$$\left(\frac{i^2}{a_0^2} + \frac{j^2}{b_0^2}\right) \cdot \lambda^2 + \left(\frac{i}{a_0} + \frac{j}{b_0}\right) \cdot 2\lambda + \left(2 - \frac{\epsilon_1 \cdot \epsilon_2}{\epsilon_1 + \epsilon_2}\right) = 0 \quad (3)$$

where λ is the wavelength. These results are plotted in Fig. 4(c). It shows the wavelength of the transmitted light (left axis) and the energy (right axis) as a function of the hole-array pitch. Two different sets of quantum numbers are shown, $(i, j) = (1, 0)$ and $(1, 1)$ for both gold–air and gold–quartz interfaces [21,22]. The comparison of Fig. 4 (b) and (c) shows a reasonable agreement. The horizontal axis along Fig. 4(b) shows the position of the holes along the device. Along this axis, the pitch changes from 350 nm to 750 nm. When comparing the transmitted wavelength to the expected one that is shown in Fig. 4(c), one can see that the spectral range is similar. The data however, does not give an exact fit, as was already shown in previous publications. This is due to the use of a rather simple model (Eqs. (1)–(3)) that does not take into account more complex effects such as the interaction of the gold–air and the gold–quartz interfaces.

In order to validate the method, a periodic object having 100 lp/mm was used. It was brought to contact with the holes array and the transmission spectrum through the system was measured at every point of the sample.

The reconstruction of the spatial data by using the single measured spectrum is performed in the following way. First, we measure the

different spectra along the long axis of the holes array, and save a set of spectra (Fig. 4(a)) in a library with the known spatial position of each spectrum. It is assumed that the transmitted spectrum at each point along the hole-array does not change when a sample is placed next to it, except for the transmitted intensity that may be reduced due to the transmission through the sample. Such a change can happen only if the index of refraction significantly changes and it is not uniform. Such an effect is highly unlikely, especially for biological samples and a rather simple test showing the uniformity of the transmitted light was shown before [21]. This spectral library can be measured only once, and it can be used as long as the hole-array does not change.

Then the sample is placed on the hole-array and a single spectrum of the light that is transmitted through the sample is measured. Note that this is a single spectrum that combines the many different spectra that are transmitted through the whole sample.

To reconstruct the object we decompose the single transmitted spectrum through the sample to the set of spectral components based on the spectral library. The decomposition is performed with a nonnegative least-squares decomposition algorithm [24] of the form $\min_x \|C \cdot x - d\|_2^2, x \geq 0$ (the “2” subscript designates that we are dealing with second order norm). C is a matrix that is built from the spectral library and each row is a single spectrum measured at a specific position along the array long axis (Fig. 4(a)). d is the measured transmitted spectrum through the objects that was illuminated using the holes array device and x is an unknown vector that is found by minimizing the equation given above. Each value in the vector x corresponds to the transmission intensity at a certain point along the hole-array, and it holds the reconstructed spatial information about the inspected object.

Note that in Fig. 4(a) spectral overlapping exists. This overlapping is equivalent to spatial blurring. However, this spectral overlapping can be overcome by an improved fabricated device. It is possible to have holes array with much sharper spectral peaks and thus with much higher spatial resolution. Narrowing the spectral peaks can be done for instance by addition of grooves in the gold plane in between the holes or by generating of structure also in the axial axis and not only in the horizontal and vertical axes.

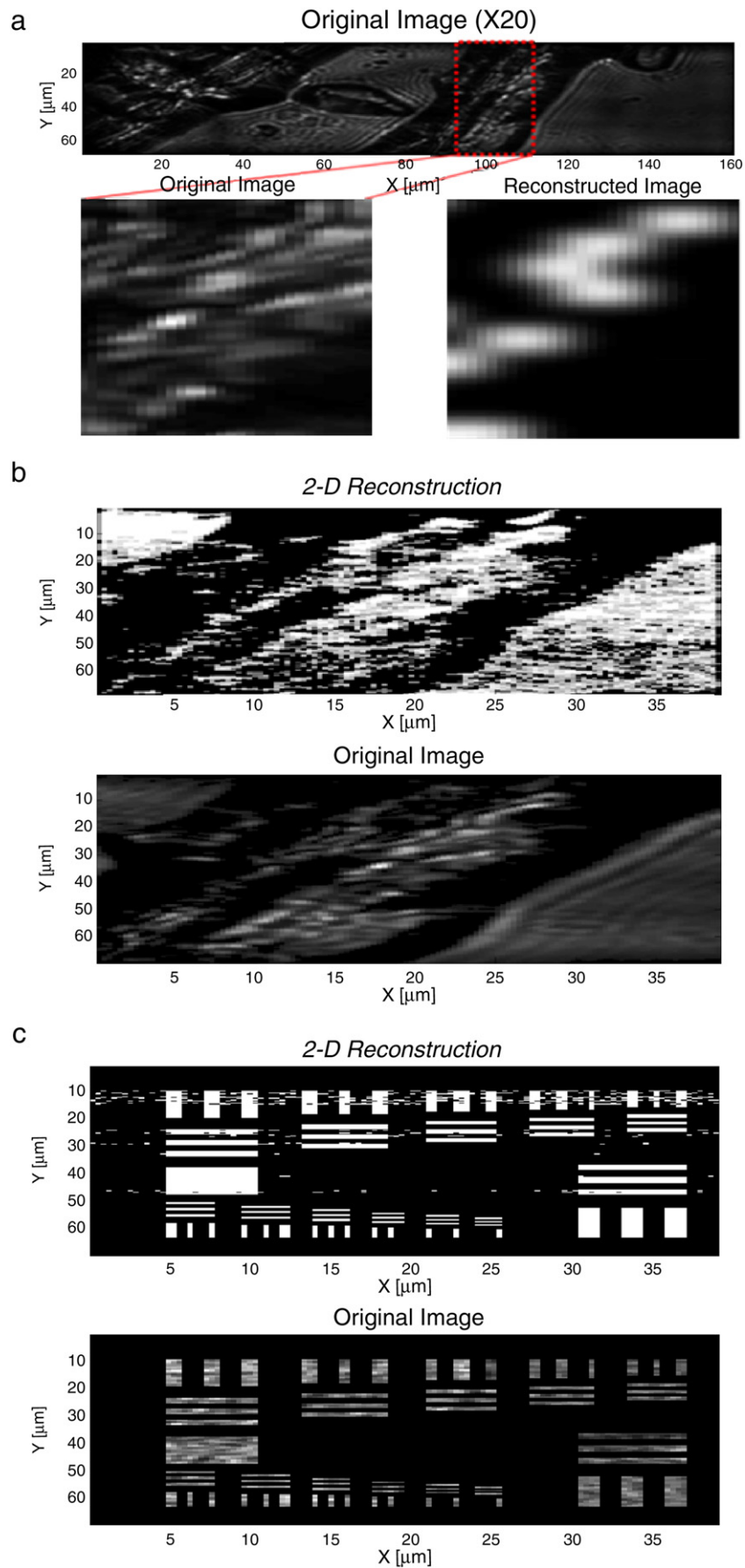


Fig. 6. (a) Experimental results including 2D mapping of 6 μm polystyrene beads. (b) Physical numerical simulation for the experimentally captured image of 6(a). (c) Physical numerical simulations for a resolution target.

In Fig. 5 we present the actual transmission intensity through the object (described above) placed in close proximity to the fabricated device. The object in this case was a grating with period of approximately 100 lp/mm. The illumination was done with conventional white light halogen lamp. The grating object was positioned about 1–2 μm from the holes array. The upper part of the figure shows the image of the grating and the lower part shows the image obtained after the reconstruction process. The reconstruction was obtained using a single transmitted spectrum through the holes array and the test-object, and the reference spectra. It was created by measuring a spectral image and summing all the spectra from all the pixels of the devices and reference spectra as explained before.

Note that in our 1D experimental reconstruction we used the entire lateral area of the fabricated element (which was approximately 60 μm by 150 μm) in order to get the average shifted spectra which relate to a different period of holes. For achieving a 2D object reconstruction without moving the element along the object we need to repeat the measurements while using each time spatial segments of only $\sim 2 \mu\text{m} \times 150 \mu\text{m}$ of the element's area. Finally we assemble all the slices into a 2D image. Specifically, the 2D image obtained from the spectrum analyzer which included wavelengths spreading over the horizontal axis and spatial information over the vertical axis, was divided into segments of 2 μm wide along the vertical axis. Each segment of 2 μm was analyzed using the algorithm described above. Thus, the horizontal resolution was limited due to the wavelengths spreading while the vertical resolution was set to 2 μm . The selection of 2 μm wide segment is due to the smallest width that could be extracted with sufficient signal to noise ratio (SNR) when using the composed numerical reconstruction algorithm (narrower spatial slices did not give sufficient SNR for the reconstruction).

Fig. 6(a) shows the testing of the proposed method for an input object which was a dry sample of LinearFlow™ Green Flow Cytometry polystyrene 6 μm beads. The upper part of Fig. 6(a) shows the reference image of the sample as it was obtained using a conventional $\times 20$ magnification objective lens. The bottom-left figure shows an enlarged (zoomed) area of the captured reference image while in the bottom-right figure one can see the reconstruction obtained using the proposed approach while using the holes array. One may clearly see the diagonal line which contains 2D features that appears both in the reference zoomed image (bottom-left) as well as in the reconstructed image (bottom-right).

Note that the current preliminary reconstructed algorithm that we have developed obtains only binary reconstruction of objects. Thus, it is capable of reconstructing the contour or the regions where the light appeared in the original object (as we did in Figs. 5 and 6(a)). Therefore, in order to obtain the non binary image as the one seen in the bottom-right part of Fig. 6(a), we convolved the binary reconstruction with the point spread function corresponding to the one of the $\times 20$ objective.

In all the experiments the exposure time of the spectrometer detector was 100 ms. The spectral range we used was 540–680 nm. The spectral resolution of the spectrometer was about 5 nm and the illuminating power of the halogen lamp reaching the holes array was approximately 1 W.

In order to further demonstrate the capabilities of the proposed approach, we simulated the proposed physical microscope system. The results are presented in Fig. 6(b) and (c). Fig. 6(b) shows the 2D reconstruction for the experimentally captured beads image from the upper part of Fig. 6(a). Fig. 6(c) shows the simulation for a resolution target. One can see that in both cases of Fig. 6(b) and (c) the reconstructed images are similar to the original high resolution images that may be obtained with regular microscope.

In the simulation we used the original data as it was experimentally obtained for the 1D experiment. The only difference was that during the experiment we place the sample under the holes array

while in this 2D simulation we used the light that was measured at the output of the array in order to illuminate the 2D sample. For the decoding of the spatial information we used the same 2D algorithm which was previously described in the paper. The only difference in numerical simulation in comparison to the 2D experimental results is that in the vertical axis we used spatial segments of 660 nm instead of 2 μm . Thus in this 2D simulation the horizontal resolution was determined by the spectral spreading done with the holes array while the vertical resolution was 660 nm.

4. Eligibility for microscopy

When extending the proposed approach to microscopy related applications several important issues should be considered. One important feature is related to 2D images. Indeed in the preliminary experimental results the 2D image was obtained by time-sequentially capturing several images while reducing the effective usable region of the element. In the general case this is not required. Currently the fabricated holes array contained a varying pitch of the holes only along one dimension which causes chromatic dispersion along one axis only. However, a similar device can be fabricated with a varying pitch in both axes such that a 2D chromatic dispersed illumination is generated. The only requirement in such a design is that the spectral encoding made by the hole element will be such that each lateral coordinate of the object will be illuminated by a different color composition, i.e. all the periods of the holes will vary in the 2D domain such that there will be no two identical periods.

Another important issue is related to the depth of focus and to the application of the proposed configuration for biological samples. From the simulations presented in Fig. 1 one may see that the diffracted pattern is preserved along an axial distance of about 10–20 μm . Therefore, the holes array does not have to be in contact with the inspected sample. It may be positioned at a distance of up to about 20 μm away which also fits well to the 3D topography of cells (or any other non flat object).

The beam diffracted from the holes array is not continuous, as light is passing only through the holes. To avoid spatial under sampling of the object, few images of the object can be measured while shifting the object with respect to the hole arrays. A small number of shifted images are enough to cover the gaps that are in between the holes. For a typical pitch of 400 nm, four shifted images would provide a spatial sampling period of ~ 100 nm.

The obtainable imaging field of view is another important parameter. It depends on the number of orthogonal transmitted spectra that can be measured by the spectrometer. Although in the proposed experiment the number was relatively low (about 40 points), it can be extended by using a broader spectral range and by using a better spectral resolution. Obviously this higher spectral resolution of the spectrometer should not be higher than the finest spectral separation generated by plasmon resonance in the holes array.

In general, the sample may not have a flat absorption or refraction curve over the entire measured spectral range. Thus, the measurement described above may give a wrong image of the measured object. To solve that, the calibration process should take it into account not only the spectral transmission of each point of the holes array, but also the spectral transmission of the sample itself. It can be measured prior to the actual spectral measurement through the holes array and sample. Only after performing this measurement, the holes array should be inserted and the spatial mapping to be performed. The decoding algorithm should take into account the spectral transmission of the inspected sample.

5. Conclusions

We presented a new microscope configuration that does not require an objective lens neither a condenser. Instead, a metallic plate

of sub-wavelength holes array with a varying pitch is used in order to illuminate the inspected object with a spectral pattern that is spatially-dependent. This illumination generates wavelength based encoding of the spatial information. During the measurement, a single spectrum is acquired with a single-point detector. The measured spectrum is then decoded using a decomposition algorithm.

The advantage of using the holes array for the encoding is that it may allow 2D encoding of a wide field of view (encoding that is obtained simultaneously without the need for temporal scanning), it allows to obtain this encoding without using a condenser lens with high resolution (i.e. high numerical aperture) as was done in Ref. [17]. The holes array is basically equivalent to a condenser lens that has very short focal length of few microns and yet very large working field.

The non periodic plate is metallic and has high energetic throughput although the holes are small in comparison to their pitch (this is a unique property that the overall energetic transmission is much larger than the overall area of the holes in the array). The high energetic throughput is obtained due to plasmon related interference effect.

Numerical simulations as well as preliminary experimental results were presented.

References

- [1] T.W. Ebbesen, H.J. Lezec, H.F. Ghaemi, T. Thio, P.A. Wolf, *Nature* 39 (1998) 667.
- [2] C. Genet, T.W. Ebbesen, *Nature* 44 (2007) 39.
- [3] M.W. Docter, I.T. Young, O.M. Piciu, A. Bossche, P.F. Alkemade, P.M. van den Berg, Y. Garini, *Opt. Express* 14 (2006) 9477.
- [4] Z. Zalevsky, A. Shemer, A. Zlotnik, E. Ben-Eliezer, E. Marom, *Opt. Exp.* 14 (2006) 2631.
- [5] Z. Zalevsky, S. Ben-Yaish, *Opt. Exp.* 15 (2007) 7202.
- [6] B. Huang, M. Bates, X. Zhuang, *Ann. Rev. Biochem.* 78 (2009) 993.
- [7] J. McDonald, *Optical Microscopy*, ASM International 0-87170-804-3, 2004.
- [8] Y. Garini, B.J. Vermolen, I.T. Young, *Curr. Opin. Biotechnology* 16 (2005) 3.
- [9] S. Bradbury, P. Evannett, *Fluorescence Microscopy, Contrast Techniques in Light Microscopy*, BIOS Scientific Publishers, Ltd., Oxford, United Kingdom, 1996.
- [10] S.W. Hell, *Nat. Biotechnol.* 21 (2003) 1347.
- [11] M.G.L. Gustafsson, *PNAS USA* 102 (2005) 13081.
- [12] M.J. Rust, M. Bates, X. Zhuang, *Nat. Methods* 3 (2006) 793.
- [13] S.T. Hess, T.P.K. Girirajan, M.D. Mason, *Biophys. J.* 91 (2006) 4258.
- [14] D.B. Shao, S.C. Chen, *Nano Lett.* 6 (2006) 2279.
- [15] A.I. Kartashev, *Opt. Spectrosc.* 9 (1960) 204.
- [16] D. Mendlovic, J. Garcia, Z. Zalevsky, E. Marom, D. Mas, C. Ferreira, A.W. Lohmann, *Appl. Opt.* 36 (1997) 8474.
- [17] A. Schwarz, A. Weiss, D. Fixler, Z. Zalevsky, V. Micó, J. García, *Opt. Commun.* 282 (2009) 2780.
- [18] X. Cui, L.M. Lee, X. Heng, W. Zhong, P.W. Sternberg, D. Psaltis, C. Yang, *PNAS USA* 105 (2008) 10670.
- [19] A.F. Coskun, I. Sencan, T.W. Su, A. Ozcan, *Opt. Express* 18 (2010) 10510.
- [20] W. Bishara, T.W. Su, A.F. Coskun, A. Ozcan, *Opt. Express* 18 (2010) 11181.
- [21] M.W. Docter, P.M.V.D. Berg, P.F.A. Alkemade, V.G. Kutchoukov, O.M. Piciu, A. Bossche, I.T. Young, Y. Garini, *J. Nanophotonics* 1 (2007) 011665.
- [22] H.F. Ghaemi, T. Thio, D.E. Grupp, T.W. Ebbesen, H.J. Lezec, *Phys. Rev. B* 58 (1998) 6779.
- [23] H. Raether, *Surface Plasmons on Smooth and Rough Surfaces and on Gratings*, Springer-Verlag, Berlin, 1988.
- [24] C.L. Lawson, R.J. Hanson, *Solving Least-Squares Problems*, Prentice-Hall, 1974, p. 161, Ch. 23.